

Structured Domain Adaptation for Unsupervised Person Re-identification

Yixiao Ge, Feng Zhu, Rui Zhao, and Hongsheng Li

The Chinese University of Hong Kong
{yxge@link,hsli@ee}.cuhk.edu.hk

Abstract. Unsupervised domain adaptation (UDA) aims at adapting the model trained on a labeled source-domain dataset to another target-domain dataset without any annotation. The task of UDA for the open-set person re-identification (re-ID) is even more challenging as the identities (classes) have no overlap between the two domains. Existing UDA methods for person re-ID have the following limitations. 1) Pseudo-label-based methods [32,29,7] achieve state-of-the-art performances but ignore the complex relations between two domains' images, along with the valuable source-domain annotations. 2) Domain translation-based methods [4,28] cannot achieve competitive performances as the domain translation is not properly regularized to generate informative enough training samples that well maintain inter-sample relations. To tackle the above challenges, we propose an end-to-end structured domain adaptation framework that consists of a novel structured domain-translation network and two domain-specific person image encoders. The structured domain-translation network can effectively transform the source-domain images into the target domain while well preserving the original intra- and inter-identity relations. The target-domain encoder could then be trained using both source-to-target translated images with valuable ground-truth labels and target-domain images with pseudo labels. Importantly, the domain-translation network and target-domain encoder are jointly optimized, improving each other towards the overall objective, *i.e.* to achieve optimal re-ID performances on the target domain. Our proposed framework outperforms state-of-the-art methods on multiple UDA tasks of person re-ID.

Keywords: Structured Domain Translation, Unsupervised Domain Adaptation, Person Re-identification

1 Introduction

Person re-identification (re-ID) aims at identifying images of the same person across multiple cameras. Despite great performance advances of recent deep learning-based re-ID methods, evident performance drops are observed when directly generalizing the trained models from one dataset (domain) to a new

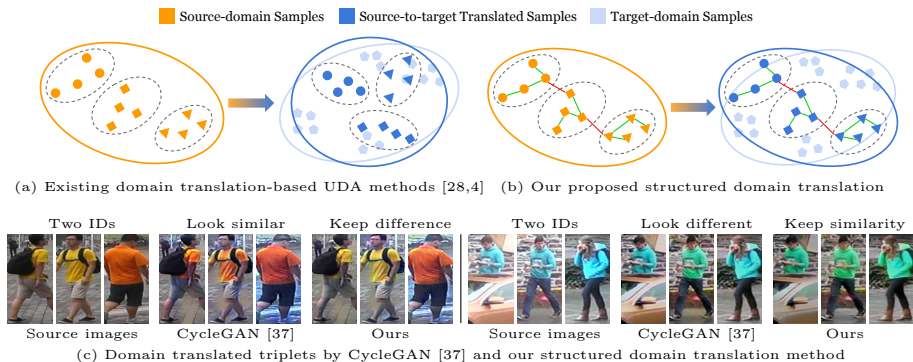


Fig. 1. (a) The source-to-target translated images in existing translation-based UDA methods cannot maintain their original inter-sample relations. (b) The intra-/inter-class relations are well maintained by our method during domain translation. (c) We illustrate two example triplets that fail to preserve the inter-person and intra-person relations without the proposed structured regularization. Source-to-target images translated by our method are more informative for improving target-domain person re-ID. Best viewed in color

dataset due to the domain gaps between different surveillance cameras. Large-scale datasets are the foundations for achieving high re-ID accuracy, however, manual labelling is generally time-consuming and labour-intensive for each new (target) domain. Unsupervised Domain Adaptation (UDA) is therefore attracting increasing attention when dealing with learning discriminative features for a new target dataset without any annotation. It aims at transferring the model’s knowledge from the labeled source domain to the unlabeled target domain.

State-of-the-art pseudo-label-based UDA methods for person re-ID [32,29,7] focus on learning target-domain person features with generated pseudo identities. They generally utilize annotated source-domain images for pre-training, and then fine-tune the models only with the target-domain images and pseudo labels. Such a pipeline simply ignores the relations between data of the two domains and wastes the valuable ground-truth identity labels in the source domain. However, directly training with different domains’ raw images actually harms the feature learning due to the large domain gaps. Therefore, carefully translating source-domain images to the target domain as additional training samples is one plausible solution, which allows jointly training the re-ID model with images of both domains and fully utilizes the source-domain ground-truth identity labels.

Previous domain translation-based UDA methods for re-ID [4,28] adopt image-to-image translation models [37] to translate source-domain images in order to have the same style as the target-domain images while remaining their original contents. By training with such domain-translated images and their ground-truth identity labels, the model is adapted to the target domain. Unfortunately, such methods have inferior performances than state-of-the-arts [32,29,7]. We argue that translation-based methods have great potentiality and their inferiority is

due to the fact that the domain-translation network in these frameworks [4,28] is only independently trained and is not optimized towards solving the final objective, *i.e.* to correctly measure similarities between target-domain person images. More importantly, the source-to-target translated images fail to maintain their original intra- and inter-identity relations and cannot act as informative training samples for the target-domain network. As illustrated in Fig. 1(a), the translated images might lose their original inter-sample relations after domain translation.

To tackle this challenge, we propose a deep end-to-end structured domain adaptation (SDA) framework that consists of a novel structured domain-translation network, a source-domain person image encoder and a target-domain person image encoder. The structured domain-translation network and the target-domain encoder are jointly optimized so that they can keep improving each other for optimal re-ID performances.

The structured domain-translation network adopts the CycleGAN [37] architecture for translating source- and target-domain images back and forth. To remedy the issue of failing to create informative target-domain training samples, we propose a novel structured regularization, called relation-consistency loss, to supervise the source-to-target domain-translation process, so that the intra- and inter-identity relations between original source-domain images should be maintained as much as possible. Such relations can be modelled by the coupledly trained source-domain and target-domain person image encoders. In Fig. 1(b), we illustrate that the inter-sample relations are well maintained after domain translation by our proposed structured domain-translation network.

Since the original relations between the source-to-target translated images can be well maintained with the proposed structured regularization, the source-to-target translated images and target-domain images can be assumed to be lied on the same image manifold within the target domain, and their associated identity labels can be constructed as a joint label system for training an improved target-domain encoder. Therefore, the target-domain encoder is able to fully explore the complex relations between both source-domain and target-domain samples, learning better feature representations for person re-ID.

The contributions of this paper could be summarized as three-fold. (1) Given observed shortcomings of translation-based UDA methods, we introduce a structured regularization to maintain the intra- and inter-identity relations during domain translation and generate more informative training samples to tackle the challenges in unsupervised person re-ID. (2) A novel structured domain adaptation (SDA) framework is proposed, where the structured domain-translation network and the target-domain person image encoder are jointly optimized and effectively improve each other to achieve the optimal re-ID performance. The structured domain-translation network provides source-to-target training samples with ground-truth identity labels to improve the target-domain encoder, which, in turn, better regularizes the structured domain translation training. (3) Our proposed SDA outperforms state-of-the-art UDA methods on person re-ID with a plain backbone network and without any additional parameters.

2 Related Work

Unsupervised domain adaptation (UDA) for person re-ID. There are two main categories for existing UDA methods on person re-ID. Pseudo-label-based methods [6,32,29,7,30,36] achieved state-of-the-art performances by modelling target-domain data distributions with generated hard or soft labels. PUL [6] proposed to learn target-domain features by self-training with hard clustering labels. SSG [29], PAST [32] and MMT [7] further explored such clustering-based methods by introducing local features, progressive training strategy and mutual mean-teaching scheme. MAR [30] assigned soft labels for unlabeled data by measuring similarities with reference images. However, such methods only focused on the target-domain data and wasted the valuable ground-truth identities in the source domain. ENC [36] used raw source- and target-domain images for jointly training but still ignored the complex relations between two domains' images, since they did not optimize two domains' images in an unified feature space with a joint label system.

Domain translation-based methods [4,28] aimed at fine-tuning the target-domain model with source-to-target translated images and their corresponding ground-truth identities. PTGAN [28] imposed pixel-level constraints on maintaining the color consistency during the domain translation. SPGAN [4] further minimized the feature-level similarities between translated images and the original ones. However, such methods failed on generating informative training samples for achieving state-of-the-art performances. That is because they only focused on ensuring each individual translated sample should preserve its original appearance in the new domain, while ignoring the consistency of inter-sample relations during the domain translation.

Unsupervised domain adaptation (UDA). Feature-level adaptation and pixel-level adaptation are mostly adopted by UDA methods for tackling more general tasks. The feature-level adaptation methods [16,24,26] aimed at aligning the feature distributions between the source and target domains by learning domain-invariant features with an domain adversarial classifier [1,26] or reducing the Maximum Mean Discrepancy (MMD) [8] distance between domains. However, such methods are not available for our open-set re-ID problem with disjoint label systems in two domains referring to [36,19,22]. The other category of pixel-level adaptation methods [11,14,3] minimized the domain shifts by translating images to the same domain, which has been widely studied in semantic segmentation tasks. However, existing pixel-level adaptation methods ignored the consistency of intra- and inter-identity relations during the domain translation process, facing the same challenge as existing translated-based UDA methods for person re-ID [4,28].

3 Structured Domain Adaptation for Unsupervised Open-set Person Re-identification

We propose a structured domain adaptation framework to tackle the challenges in unsupervised domain adaptation for person re-ID. The overall framework, as

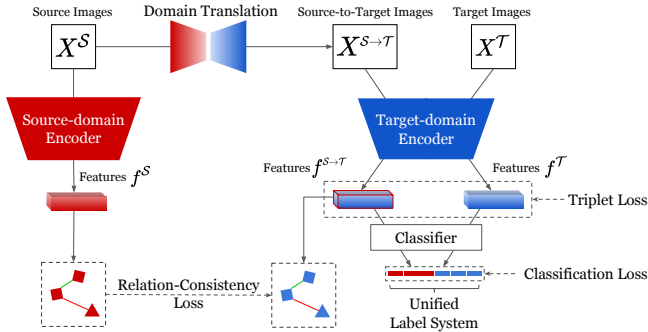


Fig. 2. Illustration of our structured domain adaptation (SDA) framework, where the structured domain-translation network and the target-domain encoder are jointly optimized to improve each other towards the final objective of accurate person re-ID

illustrated in Fig. 2, consists of a novel structured domain-translation network and two domain-specific person image encoders, which are jointly optimized.

The key innovation of the proposed structured domain-translation network lies in the creation of informative training samples by translating source-domain images into the target domain with preserved intra- and inter-identity relations, which have never been investigated in UDA methods. In this way, the generated source-to-target images with their valuable ground-truth identity labels and the target-domain images with pseudo identity labels can create a unified training set for better optimizing the target-domain image encoder. However, there is a lack of inter-sample relations in both source and target domains. We propose to use outputs of source-domain and target-domain image encoders on-the-fly to generate online inter-sample relations to regularize the proposed structured domain translation. Therefore, the structured domain translation and image encoders can be jointly optimized and assist each other to learn more discriminative person representations.

3.1 Source-domain Encoder Pre-training

We pre-train the person image encoder F^S in the source domain for (1) providing pseudo “ground-truth” inter-sample relations between source-domain images to regularize the proposed structured domain translation and (2) providing weight initialization for the target-domain person image encoder F^T . A strong encoder is the foundation of learning discriminative person features and providing valuable inter-sample relations within the two different domains. We adopt the state-of-the-art network [17] with ResNet-50 [9] as the backbone for both the source- and target-domain encoders, each of which is followed by a learnable linear classifier to predict identity labels. Given the source-domain samples X^S with ground-truth labels Y^S , the encoder F^S is trained to transform each sample $x^S \in X^S$ into a feature vector $f^S = F^S(x^S)$. If the feature vector f^S is discriminative enough, it could be used to correctly predict its ground-truth identity with the classifier $C^S : f^S \rightarrow \{1, \dots, P^S\}$, where P^S is the number of identities in the source domain. The cross-entropy classification loss and the batch-hard triplet loss [10] are adopted jointly for training,

$$\mathcal{L}_{enc}^S(F^S, C^S) = \mathcal{L}_{cls}^S(F^S, C^S) + \lambda_{tri} \mathcal{L}_{tri}^S(F^S), \quad (1)$$

where

$$\begin{aligned} \mathcal{L}_{cls}^S(F^S, C^S) &= \mathbb{E}_{x^S \sim X^S} \left[\ell_{ce}(C^S(f^S), y^S) \right], \\ \mathcal{L}_{tri}^S(F^S) &= \mathbb{E}_{x^S \sim X^S} \left[(\|f^S - f_p^S\| + m - \|f^S - f_n^S\|)^+ \right]. \end{aligned}$$

Here ℓ_{ce} denotes the cross-entropy loss for a single sample and $(\cdot)^+ = \max(0, \cdot)$ with a margin m . The subscripts p, n denote the mini-batch’s hardest positive and negative feature indexes for the sample x . λ_{tri} weights the the two losses.

After training, the source-domain F^S is frozen to provide reliable and stable inter-sample relations in the joint optimizing scheme of the proposed structured domain adaptation framework.

3.2 Structured Domain Translation

We propose a novel structured domain-translation (SDT) network to generate informative training samples by translating source-domain images X^S to the target domain \mathcal{T} , which focuses not only on image-style transfer but more on how to maintain their original intra- and inter-identity relations. The source-to-target translated images with their ground-truth labels and target-domain images with the pseudo labels can then be jointly utilized for learning to encode all the images into the target-domain embedding space. We adopt the widely-used CycleGAN [37] architecture for our translation network, which is trained to translate images along two directions, *i.e.* $\mathcal{S} \rightarrow \mathcal{T}$ and $\mathcal{T} \rightarrow \mathcal{S}$, with corresponding generators $G^{\mathcal{S} \rightarrow \mathcal{T}}$ and $G^{\mathcal{T} \rightarrow \mathcal{S}}$.

Conventional cycle generation losses. The general training objective of a CycleGAN [37] for image-to-image translation consists of the adversarial losses $\mathcal{L}_{adv}^S, \mathcal{L}_{adv}^T$, the cyclic reconstruction loss \mathcal{L}_{cyc} and the target-domain identity constraint \mathcal{L}_{id} . We adopt the loss function of LSGAN [18] with two domain discriminators D^S and D^T as

$$\begin{aligned} \mathcal{L}_{adv}^S(G^{\mathcal{T} \rightarrow \mathcal{S}}, D^S) &= \mathbb{E}_{x^S \sim X^S} \left[D^S(x^S)^2 \right] + \mathbb{E}_{x^T \sim X^T} \left[\left(D^S(G^{\mathcal{T} \rightarrow \mathcal{S}}(x^T)) - 1 \right)^2 \right], \\ \mathcal{L}_{adv}^T(G^{\mathcal{S} \rightarrow \mathcal{T}}, D^T) &= \mathbb{E}_{x^T \sim X^T} \left[D^T(x^T)^2 \right] + \mathbb{E}_{x^S \sim X^S} \left[\left(D^T(G^{\mathcal{S} \rightarrow \mathcal{T}}(x^S)) - 1 \right)^2 \right]. \end{aligned} \quad (2)$$

The cyclic reconstruction loss is adopted to supervise the pixel-level generation by translating the images twice,

$$\begin{aligned} \mathcal{L}_{cyc}(G^{\mathcal{S} \rightarrow \mathcal{T}}, G^{\mathcal{T} \rightarrow \mathcal{S}}) &= \mathbb{E}_{x^S \sim X^S} \left[\|G^{\mathcal{T} \rightarrow \mathcal{S}}(G^{\mathcal{S} \rightarrow \mathcal{T}}(x^S)) - x^S\|_1 \right] \\ &\quad + \mathbb{E}_{x^T \sim X^T} \left[\|G^{\mathcal{S} \rightarrow \mathcal{T}}(G^{\mathcal{T} \rightarrow \mathcal{S}}(x^T)) - x^T\|_1 \right]. \end{aligned} \quad (3)$$

The identity consistency loss [37,28,4] maintains the appearances as,

$$\begin{aligned} \mathcal{L}_{id}(G^{\mathcal{S} \rightarrow \mathcal{T}}, G^{\mathcal{T} \rightarrow \mathcal{S}}) &= \mathbb{E}_{x^S \sim X^S} \left[\|G^{\mathcal{T} \rightarrow \mathcal{S}}(x^S) - x^S\|_1 \right] \\ &\quad + \mathbb{E}_{x^T \sim X^T} \left[\|G^{\mathcal{S} \rightarrow \mathcal{T}}(x^T) - x^T\|_1 \right]. \end{aligned} \quad (4)$$

Despite the fact that the above regularizations translate the source-domain images to have target-domain image style, the generated images generally fail to maintain their original intra- and inter-class relations and are therefore not accurate enough to supervise the target-domain image encoder (see Fig. 1(c)).

Relation-consistency Loss. One of the key tasks of the proposed structured domain translation is to transform source-domain images to have the target-domain style while preserving their original inter-sample relations. Since the identity labels in the source domain alone are not enough to provide accurate inter-sample relations, we propose to use the trained and fixed source-domain image encoder F^S to provide inter-sample relation supervisions, which are modelled as “soft” softmax-triplets.

Given a source-domain image $x^S \in X^S$, its positive sample $x_p^S \in X^S$ with the same identity, and its negative sample $x_n^S \in X^S$ with a different identity, we can measure the intra-/inter-identity relations among the triplet with the softmax-triplet function [31] as

$$\mathcal{R}(x^S; F^S) = \frac{\exp\langle f^S, f_p^S \rangle}{\exp\langle f^S, f_p^S \rangle + \exp\langle f^S, f_n^S \rangle}, \quad (5)$$

where f^S , f_p^S , f_n^S are the encoded feature representations by the pre-trained source-domain encoder F^S on the image samples x^S , x_p^S , x_n^S , respectively, and $\langle \cdot, \cdot \rangle$ is the dot product between two feature vectors to measure their similarity. Similar to [10], we utilize only the most difficult triplet of each sample x^S within a batch, *i.e.* the hardest positive and negative samples for each x^S .

After translating source-domain images to the target domain by $G^{S \rightarrow T}$, we obtain the features of the source-to-target translated triplet $f^{S \rightarrow T}$, $f_p^{S \rightarrow T}$, $f_n^{S \rightarrow T}$, which is encoded by the target-domain encoder F^T (to be discussed in Section 3.3). Similarly, the relation between the translated images can still be calculated by the softmax-triplet function [31] as

$$\mathcal{R}(x^S; G^{S \rightarrow T}, F^T) = \frac{\exp\langle f^{S \rightarrow T}, f_p^{S \rightarrow T} \rangle}{\exp\langle f^{S \rightarrow T}, f_p^{S \rightarrow T} \rangle + \exp\langle f^{S \rightarrow T}, f_n^{S \rightarrow T} \rangle}, \quad (6)$$

We argue that, if the domain-translation network well preserves the source-domain images’ identities and their inter-sample relations, their softmax-triplet function responses should be similar. Based on this assumption, a novel relation-consistency loss is introduced to regularize the inter-sample relations before and after the translation $\mathcal{S} \rightarrow \mathcal{T}$ as

$$\mathcal{L}_{rc}(G^{S \rightarrow T}) = \mathbb{E}_{x^S \sim X^S} \left[\ell_{bce} \left(\mathcal{R}(x^S; G^{S \rightarrow T}, F^T), \mathcal{R}(x^S; F^S) \right) \right], \quad (7)$$

where $\ell_{bce}(\hat{y}, y) = -y \log \hat{y} - (1 - y) \log (1 - \hat{y})$ is the binary cross-entropy loss. We use the source-domain inter-sample relations in Eq. (5) as soft supervisions for supervising the translated inter-sample relations in Eq. (6).

During training, we fix the source-domain encoder F^S and alternatively optimize F^T and $G^{S \rightarrow T}$ to avoid bias amplification. When fixing F^T , \mathcal{L}_{rc} focuses on regularizes the domain translation networks $G^{S \rightarrow T}$ to maintain inter-sample relations. When fixing $G^{S \rightarrow T}$, it generates additional training samples to more effectively train the target-domain image encoder F^T . Once F^T is further trained to achieve better re-ID performance on the target domain, it could in turn measure more accurate data relations for further improving the structured domain-translation network $G^{S \rightarrow T}$ via \mathcal{L}_{rc} .

The SDT network is optimized with the following joint objective function,

Algorithm 1 Structured Domain Adaptation for Unsupervised Person Re-ID

Require: Source-domain data X^S with label set Y^S , target-domain data X^T ;

Require: Weighting factors $\lambda_{rc}, \lambda_{cyc}, \lambda_{adv}, \lambda_{id}$ for Eq. (8), λ_{tri} for Eqs. (1), (9);

```

1: Pre-train source-domain encoder  $F^S$  by minimizing Eq. (1) on  $X^S$ ;
2: for  $n$  in  $[1, num\_epochs]$  do
3:   Create pseudo label set  $\hat{Y}^T$  by clustering  $F^T(X^T)$ ;
4:   for each mini-batch  $B^S \subset X^S, B^T \subset X^T$  do
5:     Translate  $B^S$  into the target domain as  $B^{S \rightarrow T}$  by  $G^{S \rightarrow T}$ ;
6:     Update  $G^{S \rightarrow T}, G^{T \rightarrow S}$  by minimizing the objective function Eq. (8) with  $D^S, D^T$  fixed,
       where the inter-sample relations are measured by  $F^S$  and  $F^T$  on-the-fly;
7:     Update  $F^T$  by minimizing the objective function Eq. (9) with  $B^{S \rightarrow T} \cup B^T$ ;
8:     Update  $D^S, D^T$  by maximizing the objective function Eq. (8) with  $G^{S \rightarrow T}, G^{T \rightarrow S}$  fixed.
9:   end for
10: end for

```

$$\begin{aligned} \mathcal{L}_{sdt}(G^{S \rightarrow T}, G^{T \rightarrow S}, D^S, D^T) &= \lambda_{rc} \mathcal{L}_{rc}(G^{S \rightarrow T}) + \lambda_{cyc} \mathcal{L}_{cyc}(G^{S \rightarrow T}, G^{T \rightarrow S}) \\ &\quad + \lambda_{adv} \left(\mathcal{L}_{adv}^S(G^{T \rightarrow S}, D^S) + \mathcal{L}_{adv}^T(G^{S \rightarrow T}, D^T) \right) + \lambda_{id} \mathcal{L}_{id}(G^{S \rightarrow T}, G^{T \rightarrow S}), \end{aligned} \quad (8)$$

where $\lambda_{rc}, \lambda_{cyc}, \lambda_{adv}$ and λ_{id} are the weighting factors for different loss terms.

3.3 Target-domain Encoder Training with Translated Images

The proposed structured domain-translation network and the target-domain person image encoder could continually improve each other by jointly training to achieve optimal re-ID performances in an end-to-end manner.

For training the target-domain encoder F^T , we collect the source-to-target translated image set $X^{S \rightarrow T}$ and the target-domain image set X^T to form a unified image set as $X^{S \rightarrow T} \cup X^T$. The source-to-target translated images can maintain their original identities Y^S . For the target domain, we perform image clustering, similar to clustering-based methods [32,29,7], to obtain pseudo labels by performing clustering on target-domain images. Based on the encoded features¹ $F^T(X^T)$, target-domain samples X^T are clustered into \hat{P}^T classes and images within the same cluster are assigned the same target-domain pseudo labels to create the label set \hat{Y}^T . Note that the clustering-based pseudo label creation was widely adopted in [32,29,7] and is not the focus of our method. Any common clustering methods can be adopted here (*e.g.* k -means, DBSCAN [5]). In this way, we can create a unified training image set $X^{S \rightarrow T} \cup X^T$ with its associated unified label set $Y^{S \rightarrow T} \cup \hat{Y}^T$ within the target domain, as well as a unified classifier $C^T: f \rightarrow \{1, \dots, P^S + \hat{P}^T\}$.

The target domain encoder F^T can then be trained in a fully-supervised manner. Specifically, each sample $x \in X^{S \rightarrow T} \cup X^T$ is assigned a corresponding label $y \in Y^S \cup \hat{Y}^T$. The target-domain person image encoder can therefore be optimized with the objective function similar to Eq. (1),

$$\mathcal{L}_{enc}^T(F^T, C^T) = \mathcal{L}_{cls}^T(F^T, C^T) + \lambda_{tri} \mathcal{L}_{tri}^T(F^T). \quad (9)$$

The target-domain encoder F^T can therefore take full advantages of (1) the source-to-target images translated by our $G^{S \rightarrow T}$, which better maintain their

¹ In the 1st epoch, the source-domain encoder F^S is used to encode target-domain image features for clustering.

intra-/inter-identity relations, and (2) the unified target-domain label set that consists of both the valuable ground-truth source-domain identity labels and the target-domain pseudo labels. F^T trained by this strategy is shown to embed more discriminative features for distinguishing target-domain identities. The structured domain-translation network and the target-domain image encoder can effectively promote each other in the joint framework, as summarized in Alg. 1. After training, only F^T is adopted to encode target-domain samples into features for ranking without additional parameters.

4 Experiments

4.1 Datasets

We evaluate our framework on three widely used person re-ID datasets, including DukeMTMC-reID [21], Market-1501 [33] and MSMT17 [28]. DukeMTMC-reID [21] contains 36,411 images of 702 identities for training and another 702 identities for testing, with all the images captured from 8 cameras. Market-1501 [33] consists of 12,936 images of 751 identities for training and 19,281 images of 750 identities for testing, which are shot by 6 cameras. MSMT17 [28] is the most challenging dataset with 126,441 images of 4,101 identities from 15 cameras, where 1,041 identities are used for training. Mean average precision (mAP) and CMC top-1/5/10 accuracies are utilized for evaluation.

4.2 Implementation Details

Training data organization. For our joint training strategy, each mini-batch contains 56 source-domain images of 8 ground-truth identities (7 for each identity) and 56 target-domain images of 8 pseudo identities. The pseudo identities are assigned by clustering algorithm and updated before each epoch. All images are resized to 256×128 , and random perturbations are applied to each image, *e.g.* randomly erasing [34], cropping and flipping.

Hyper-parameters. We tune the hyper-parameters of the proposed framework on the task of Duke→Market, and the chosen hyper-parameters are directly applied to all the other tasks. ADAM optimizer is adopted to optimize the networks with weighting factors $\lambda_{tri} = 1$, $\lambda_{rc} = 1$, $\lambda_{adv} = 1$, $\lambda_{cyc} = 10$, $\lambda_{id} = 0.5$ and the triplet margin $m = 0.3$. The initial learning rates (lr) are set to 0.00035 for person image encoders and 0.0002 for the structured domain-translation (SDT) network. The source-domain pre-training iterates for 30 epochs and the learning rate decreases to 1/10 of its previous value every 10 epochs. The proposed joint training scheme (Alg. 1) iterates for 50 epochs, where the learning rate is constant for the first 25 epochs and then gradually decreases to 0 for another 25 epochs following the formula $lr = lr \times (1.0 - \max(0, epoch - 25)/25)$. In addition, we adopt a temporally averaged model [25], denoted as F_*^T , for further stabilizing the jointly training procedure. In particular, we denote the parameters of F^T and F_*^T as $\theta^{(t)}$ and $\theta_*^{(t)}$ at iteration t . $\theta_*^{(t)}$ can be calculated as $\theta_*^{(t)} = \alpha \theta_*^{(t-1)} + (1 - \alpha) \theta^{(t)}$, where $\theta_*^{(0)} = \theta^{(0)}$ and $\alpha = 0.999$ is the ensembling momentum. F_*^T is utilized to replace F^T in Eq. (6) for measuring the feature

Table 1. Unsupervised person re-ID performances by state-of-the-art methods and our proposed SDA on DukeMTMC-reID [21], Market-1501 [33] and MSMT17 [28] datasets

Methods	Duke→Market				Market→Duke			
	mAP	top-1	top-5	top-10	mAP	top-1	top-5	top-10
PUL [6] (TOMM'18)	20.5	45.5	60.7	66.7	16.4	30.0	43.4	48.5
TJ-AIDL [27] (CVPR'18)	26.5	58.2	74.8	81.1	23.0	44.3	59.6	65.0
SPGAN [4] (CVPR'18)	22.8	51.5	70.1	76.8	22.3	41.1	56.6	63.0
HHL [35] (ECCV'18)	31.4	62.2	78.8	84.0	27.2	46.9	61.0	66.7
CFSM [2] (AAAI'19)	28.3	61.2	-	-	27.3	49.8	-	-
BUC [15] (AAAI'19)	38.3	66.2	79.6	84.5	27.5	47.4	62.6	68.4
ARN [13] (CVPR'18-WS)	39.4	70.3	80.4	86.3	33.4	60.2	73.9	79.5
UDAP [23] (Arxiv'18)	53.7	75.8	89.5	93.2	49.0	68.4	80.1	83.5
ENC [36] (CVPR'19)	43.0	75.1	87.6	91.6	40.4	63.3	75.8	80.4
UCDA [20] (ICCV'19)	30.9	60.4	-	-	31.0	47.7	-	-
PDA-Net [12] (ICCV'19)	47.6	75.2	86.3	90.2	45.1	63.2	77.0	82.5
PCB-PAST [32] (ICCV'19)	54.6	78.4	-	-	54.3	72.4	-	-
SSG [29] (ICCV'19)	58.3	80.0	90.0	92.4	53.4	73.0	80.6	83.2
MMT (dual ResNet-50's) [7] (ICLR'20)	71.2	87.7	94.9	96.9	65.1	78.0	88.8	92.5
Our SDA w/ k -means	66.4	86.4	93.1	95.6	56.7	74.0	84.1	87.7
Our SDA w/ DBSCAN	70.0	86.9	94.4	96.3	61.4	76.5	86.6	89.7
Our SDA w/ k -means + MMT [7]	74.3	89.7	95.9	97.4	66.7	79.9	89.1	92.7

Methods	Market→MSMT				Duke→MSMT			
	mAP	top-1	top-5	top-10	mAP	top-1	top-5	top-10
PTGAN [28] (CVPR'18)	2.9	10.2	-	24.4	3.3	11.8	-	27.4
ENC [36] (CVPR'19)	8.5	25.3	36.3	42.1	10.2	30.2	41.5	46.8
SSG [29] (ICCV'19)	13.2	31.6	-	49.6	13.3	32.2	-	51.2
MMT (dual ResNet-50's) [7] (ICLR'20)	22.9	49.2	63.1	68.8	23.3	50.1	63.9	69.8
Our SDA w/ k -means	20.6	46.8	59.9	65.0	23.0	51.7	64.2	69.6
Our SDA w/ DBSCAN	23.2	49.5	62.2	67.7	25.6	54.4	66.4	71.3
Our SDA w/ k -means + MMT [7]	29.0	57.0	69.5	74.1	30.3	59.6	71.7	76.2

similarities. Intuitively, the temporally averaged model could provide more reliable inter-sample relations since it eases the training bias caused by unstable translation results and noisy pseudo labels. During inference, we also adopt superior F_*^T to encode person image features for ranking.

4.3 Comparison with State-of-the-arts

We compare our proposed SDA framework with state-of-the-art methods on four domain adaptations tasks in Tab. 1, *i.e.* Duke→Market, Market→Duke, Duke→MSMT and Market→MSMT. Our proposed SDA is plug-and-play without limitation to any clustering algorithms. We tested k -means and DBSCAN [5] clustering algorithms with our proposed SDA, which were commonly used in previous clustering-based UDA methods [32,29,7]. We adopt the same clustering hyper-parameters for DBSCAN as [32,29] and select the optimal k value of k -means following the state-of-the-art [7], *i.e.* 500 for Duke→Market, 700 for Market→Duke, 1500 for Duke→MSMT and Market→MSMT. Actually, our SDA is consistently effective without the need of setting the class number to be exactly the same as the identity numbers. As shown in Tab. 3, even with different k 's, our SDA stably improves the already strong baselines, where the *baseline* model is trained with only the target-domain samples and pseudo labels.

With a plain ResNet-50 backbone, our SDA (“Our SDA w/ DBSCAN”) significantly surpasses the best-performing single-model UDA methods SSG [29] and PCB-PAST [32] which adopt the same backbone, showing noticeable 11.7%, 7.1%, 10.0% and 12.3% improvements in terms of mAP. Note that we do not split the whole-body features into multiple body parts with additional parameters as [32,29] do. Our gains are rooted in the fact that the complex relations between

Table 2. Ablation studies for our proposed framework on individual components. We report the performances when adopting k -means clustering algorithm for fast training

Methods	Duke→Market				Market→Duke			
	mAP	top-1	top-5	top-10	mAP	top-1	top-5	top-10
Pre-trained (Source \mathcal{S} Only)	21.7	47.8	64.2	70.1	14.4	26.7	39.8	45.6
Baseline (Target \mathcal{T} Only)	59.0	80.7	90.5	93.4	50.1	68.2	79.2	82.7
Baseline + Raw Source \mathcal{S}	53.2	77.5	88.9	92.1	50.8	69.1	80.1	83.1
Baseline + $\mathcal{S} \rightarrow \mathcal{T}$ by CycleGAN [37]	56.0	79.6	90.6	93.9	51.2	69.5	80.4	83.5
Baseline + $\mathcal{S} \rightarrow \mathcal{T}$ by SPGAN [4]	49.6	77.3	89.6	92.8	36.9	54.3	68.4	73.6
Baseline + $\mathcal{S} \rightarrow \mathcal{T}$ by our SDT	61.3	83.3	91.8	93.9	54.3	71.6	82.0	85.6
Our SDA w/o relation-consistency loss \mathcal{L}_{rc}	63.0	84.3	92.9	95.2	52.9	69.8	81.3	84.5
Our SDA w/o unified label system	64.8	86.0	93.1	95.2	54.8	73.1	83.1	85.5
Our SDA w/o temporally averaged model [25]	65.3	86.1	93.1	95.3	55.3	72.5	82.8	85.5
Our SDA	66.4	86.4	93.1	95.6	56.7	74.0	84.1	87.7

Table 3. Comparison with different values of k in our SDA when adopting k -means on Market→Duke

K value	Baseline (\mathcal{T} Only)		Our SDA	
	mAP	top-1	mAP	top-1
500	46.7	65.9	53.8(+7.1)	70.6(+4.7)
700	50.1	68.2	56.7(+6.6)	74.0(+5.8)
900	48.9	66.6	56.0(+7.1)	72.9(+6.3)

Table 4. Comparison with the optional ID/relation-consistency regularizations in our SDA with k -means

Methods	Duke→Market		Market→Duke	
	mAP	top-1	mAP	top-1
ID-consistency	63.3	84.5	54.3	71.1
Batch-wise	64.6	86.0	54.6	71.5
Our SDA	66.4	86.4	56.7	74.0

the two domains’ images are fully explored. Although the state-of-the-art MMT [7] shows superior performances over our single SDA model by adopting dual networks with two times more parameters for mutual training, our SDA is compatible with it and can be further improved when combined with MMT, *i.e.* we add the mutual mean-teaching strategy along with the soft-label losses introduced by MMT. The combination shows further 4.3% and 5.3% mAP gains on Duke→Market and Market→Duke respectively (see “Our SDA+MMT [7]” in Tab. 1). Also, the focus of our SDA is on structured domain translation rather than pseudo label refinery as the above mentioned [32,29,7]. Existing domain translation-based methods [28,4] show uncompetitive performances since their domain-translation networks fail to generate informative training samples without our relation-consistency loss and ignore the valuable relations between the two domains’ images. Our SDA effectively remedies such weaknesses.

4.4 Ablation Studies

We conduct ablation studies on Duke→Market and Market→Duke tasks to analyse the effectiveness of our proposed framework, where k -means is adopted here for faster training. We illustrate quantitative results in Figs. 3 and 4, and show the detailed ablation experiments in Tab. 2.

Do we need source-domain images for target-domain training? We denote the target-domain image encoder F^T independently trained with only unlabeled target-domain images and pseudo labels as our *baseline* model, which ignores the valuable ground-truth identities in the source domain. This is the common strategy adopted by existing clustering-based UDA methods [32,7]. As illustrated in Fig. 3, we compare the unsupervised re-ID performances between the baseline model “Baseline (Target Only)” and our method “Our SDA”. Our

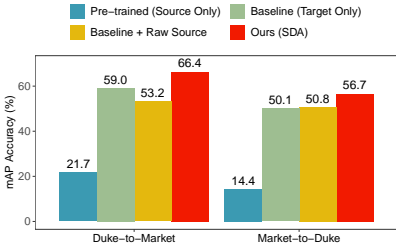


Fig. 3. Investigation on jointly training with source-to-target translated images and target-domain images

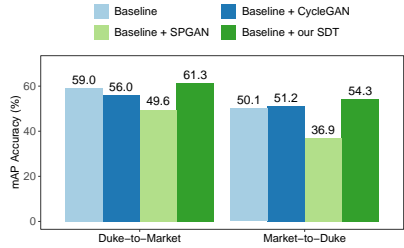


Fig. 4. Investigation on effects of maintaining inter-sample relations during domain translation



Fig. 5. Domain-translated examples of CycleGAN [37], SPGAN [4] and our SDT network. Best viewed in color

method significantly outperforms the baseline on both Duke \rightarrow Market and Market \rightarrow Duke tasks by 7.4% and 6.6% mAP improvements respectively. Comparing CMC accuracies in Tab. 2, we observe 5.7% and 5.8% improvements over the baseline in terms of top-1 on the two tasks.

The necessity of domain translation. A naïve way to use source-domain images is to directly train with two domain’s original images. We conduct such experiments, namely “Baseline+Raw Source”, by constructing a unified label system for jointly optimizing with source- and target-domain images. As shown in Fig. 3, directly training with different domains’ images performs worse than the baseline on Duke \rightarrow Market and slightly better than the baseline on Market \rightarrow Duke. This phenomenon indicates that the large domain gaps harm the feature learning since the encoder might focus on distinguishing distinct domains instead of different identities, which motivates us to adopt domain-translation networks for translating source-domain images into the target domain. Our method structuredly translates source-domain images and outperforms “Baseline+Raw Source” by 13.2% and 8.9% in terms of mAP and top-1 on Duke \rightarrow Market task (see Tab. 2). The comparison validates the necessity of jointly training with source-to-target translated images and target-domain images.

Importance of maintaining inter-sample relations during domain translation. In order to generate informative training samples, we propose to maintain the intra-/inter-identity relations among source-to-target translated im-

ages with our novel structured domain-translation (SDT) network. We conduct a series of comparison experiments without such structured regularization to validate the importance of our proposed relation-consistency loss, *i.e.* “Baseline+CycleGAN [37]”, “Baseline+SPGAN [4]”, “Baseline+our SDT”. In order to use the off-the-shelf generated images provided by SPGAN [4], the above three experiments are not optimized with our proposed jointly training strategy as introduced in Alg. 1 for fair comparison. Specifically, we independently update the target-domain encoder with off-the-shelf source-to-target translated images generated by fixed domain-translation networks. As shown in Fig. 4, “Baseline+CycleGAN [37]” slightly outperforms the baseline on the Market→Duke task. Unfortunately, “Baseline+SPGAN [4]” shows the worst performances in all three experiments. In contrast, source-to-target translated images by our proposed structured domain-translation (SDT) network successfully boosts the baseline model by 2.3% and 4.2% improvements in terms of mAP on two UDA settings. We also illustrate the translated person images by the above three experiments in Fig. 5, which are used as additional training samples for the target-domain encoder. Obviously, our method generates more informative person images by well preserving the inter-sample relations.

Besides, we also need to evaluate the contribution of the relation-consistency loss \mathcal{L}_{rc} in our overall framework. We perform an experiment by removing \mathcal{L}_{rc} , dubbed “Ours w/o \mathcal{L}_{rc} ” in Tab. 2. Different from “Baseline+CycleGAN [37]”, “Ours w/o \mathcal{L}_{rc} ” optimizes the domain-translation network and the image encoder following the proposed jointly training scheme. Referring to Tab. 2, we observe significant mAP decreases of 3.4%, 3.8%, and top-1 drops of 2.1%, 4.2% on Duke→Market and Market→Duke tasks. The designed comparisons fully demonstrate the effectiveness of preserving inter-sample relations during translation, which is ignored by existing domain translation-based UDA methods [4,28].

Comparison with optional ID/Relation-preserving regularizations. Besides the above discussion on the necessity of preserving inter-sample relations, we further explore an ID-preserving regularization and an optional relation-preserving regularization (Tab. 4) to verify the legitimacy of our well-designed inter-sample relation constraint in Eq. (7).

Adapted from [3], we design an ID-consistency loss to replace the relation-consistency loss Eq. (7) in our SDA, ensuring that each individual image in the source domain should maintain the same class prediction after source-to-target translation. The loss function is formulated as $\mathcal{L}_{ic}(G^{S \rightarrow T}) = \mathbb{E}_{x^S \sim X^S}[-C^S(f^S) \cdot \log(C^T(f^{S \rightarrow T}))]$. As shown in Tab. 4, evident 3.1% and 2.4% mAP drops are observed on two datasets, which sufficiently indicate the importance of inter-sample relation preserving in the domain translation process.

Besides our \mathcal{L}_{rc} in Eq. (7) which aims at preserving similarity-based relations within hardest triplets, we introduce an optional relation-consistency loss to preserve similarity-based relations within batches. We model the inter-sample relations by measuring the similarity vector $\mathcal{R}(x^S; F^S) = [\langle f^S, f_1^S \rangle, \dots, \langle f^S, f_k^S \rangle]$, which consists of pairwise dot products between each sample x^S and all the other ones in the same batch. The similarity vector is normalized to take batch-wise

data distributions into consideration, and a soft cross-entropy loss is adopted to regularize such relations within different domains, which is formulated as $\mathcal{L}_{brc}(G^{S \rightarrow T}) = \mathbb{E}_{x^S \sim X^S} [-\mathcal{R}(x^S; F^S) \cdot \log \mathcal{R}(x^S; G^{S \rightarrow T}, F^T)]$. The difference between \mathcal{L}_{brc} and \mathcal{L}_{rc} (Eq. (7)) is that \mathcal{L}_{brc} models the relations between the anchor and all other samples in the batch, while \mathcal{L}_{rc} focuses on the hardest positive and negative pairs. 1.8% mAP drops on Duke→Market and 2.1% mAP drops on Market→Duke are found when replacing \mathcal{L}_{rc} with \mathcal{L}_{brc} (see Tab. 4).

Effectiveness of jointly training. We propose to jointly optimize the domain-translation network and the person image encoder towards the final objective, which is ignored by existing translation-based UDA methods for person re-ID [4,28]. To evaluate the introduced training strategy in Alg. 1, two groups of comparisons are performed and reported in Tab. 2, one being “Our SDA” v.s. “Baseline+our SDT”, the other one being “Ours w/o \mathcal{L}_{rc} ” v.s. “Baseline+CycleGAN [37]”. The only variable within two sets of experiments is whether to adopt the jointly training scheme. We observe that the models always benefit from joint optimization regardless of \mathcal{L}_{rc} . Especially on the Duke→Market, considerable declines of 5.1% and 7.0% mAP are observed compared to independently training the domain-translation network and the person image encoder.

Effectiveness of training with the unified label set. We argue that the target-domain encoder benefits from the unified label set $Y^S \cup \hat{Y}^T$ by training the classifier to predict the correct label out of overall $P^S + \hat{P}^T$ classes. To verify this claim, we design an experiment with separate classifiers for source-to-target translated images and target-domain images, *i.e.* $C^T : f \rightarrow \{1, \dots, P^S + \hat{P}^T\}$ is split into $C^{S \rightarrow T} : f \rightarrow \{1, \dots, P^S\}$ and $C^T : f \rightarrow \{1, \dots, \hat{P}^T\}$. We report the performance in Tab. 2 as “Ours w/o unified label system”. 1.6%, 1.9% mAP drops are observed in the two tasks, which indicates the effectiveness of training with an unified label set in modelling the relations between two domains’ images.

Further benefits from the temporally averaged model. As described in Sec. 4.2, we utilize a temporally averaged model [25] for more stable training and better performance. To verify that the main contribution is not from such existing technique, we perform an experiment by removing the averaged model while remaining all other components. The experimental results are denoted as “Ours w/o temporally averaged model [25]” in Tab. 2. We observe slight drops of 1.1% and 1.4% in terms of mAP on two datasets.

5 Conclusion

In this work, we propose an end-to-end structured domain adaptation framework that consists of a novel structured domain-translation network and two domain-specific person image encoders to tackle unsupervised person re-ID. The domain-translation network translates the source-domain images into the target domain while well maintaining the original inter-sample relations. The source-to-target translated images and the target-domain images are jointly trained to improve the target-domain encoder, which could in turn provide more reliable relations for regularizing the translation network. Such two modules are jointly optimized towards achieving optimal re-ID performance on the target domain. Our framework outperforms state-of-the-art methods on four UDA tasks.

References

1. Bousmalis, K., Trigeorgis, G., Silberman, N., Krishnan, D., Erhan, D.: Domain separation networks. In: NIPS (2016)
2. Chang, X., Yang, Y., Xiang, T., Hospedales, T.M.: Disjoint label space transfer learning with common factorised space. AAAI (2019)
3. Chen, Y.C., Lin, Y.Y., Yang, M.H., Huang, J.B.: Crdoco: Pixel-level domain transfer with cross-domain consistency. In: CVPR. pp. 1791–1800 (2019)
4. Deng, W., Zheng, L., Ye, Q., Kang, G., Yang, Y., Jiao, J.: Image-image domain adaptation with preserved self-similarity and domain-dissimilarity for person re-identification. In: CVPR (2018)
5. Ester, M., Kriegel, H.P., Sander, J., Xu, X., et al.: A density-based algorithm for discovering clusters in large spatial databases with noise. In: Kdd. vol. 96, pp. 226–231 (1996)
6. Fan, H., Zheng, L., Yan, C., Yang, Y.: Unsupervised person re-identification: Clustering and fine-tuning (2018)
7. Ge, Y., Chen, D., Li, H.: Mutual mean-teaching: Pseudo label refinery for unsupervised domain adaptation on person re-identification. In: International Conference on Learning Representations (2020)
8. Gretton, A., Borgwardt, K., Rasch, M., Schölkopf, B., Smola, A.J.: A kernel method for the two-sample-problem. In: NIPS (2007)
9. He, K., Zhang, X., Ren, S., Sun, J.: Deep residual learning for image recognition. In: CVPR (2016)
10. Hermans, A., Beyer, L., Leibe, B.: In defense of the triplet loss for person re-identification. arXiv preprint arXiv:1703.07737 (2017)
11. Hoffman, J., Tzeng, E., Park, T., Zhu, J.Y., Isola, P., Saenko, K., Efros, A.A., Darrell, T.: Cycada: Cycle-consistent adversarial domain adaptation. ICML (2018)
12. Li, Y.J., Lin, C.S., Lin, Y.B., Wang, Y.C.F.: Cross-dataset person re-identification via unsupervised pose disentanglement and adaptation. ICCV (2019)
13. Li, Y.J., Yang, F.E., Liu, Y.C., Yeh, Y.Y., Du, X., Frank Wang, Y.C.: Adaptation and re-identification network: An unsupervised deep transfer learning approach to person re-identification. In: CVPRW (2018)
14. Li, Y., Yuan, L., Vasconcelos, N.: Bidirectional learning for domain adaptation of semantic segmentation. In: CVPR. pp. 6936–6945 (2019)
15. Lin, Y., Dong, X., Zheng, L., Yan, Y., Yang, Y.: A bottom-up clustering approach to unsupervised person re-identification. In: AAAI (2019)
16. Long, M., Cao, Y., Wang, J., Jordan, M.I.: Learning transferable features with deep adaptation networks. arXiv preprint arXiv:1502.02791 (2015)
17. Luo, H., Gu, Y., Liao, X., Lai, S., Jiang, W.: Bag of tricks and a strong baseline for deep person re-identification. In: CVPRW (2019)
18. Mao, X., Li, Q., Xie, H., Lau, R.Y., Wang, Z., Paul Smolley, S.: Least squares generative adversarial networks. In: ICCV. pp. 2794–2802 (2017)
19. Panareda Busto, P., Gall, J.: Open set domain adaptation. In: ICCV. pp. 754–763 (2017)
20. Qi, L., Wang, L., Huo, J., Zhou, L., Shi, Y., Gao, Y.: A novel unsupervised camera-aware domain adaptation framework for person re-identification. ICCV (2019)
21. Ristani, E., Solera, F., Zou, R., Cucchiara, R., Tomasi, C.: Performance measures and a data set for multi-target, multi-camera tracking. In: ECCVW (2016)
22. Saito, K., Yamamoto, S., Ushiku, Y., Harada, T.: Open set domain adaptation by backpropagation. In: ECCV. pp. 153–168 (2018)

23. Song, L., Wang, C., Zhang, L., Du, B., Zhang, Q., Huang, C., Wang, X.: Unsupervised domain adaptive re-identification: Theory and practice. arXiv preprint arXiv:1807.11334 (2018)
24. Sun, B., Saenko, K.: Deep coral: Correlation alignment for deep domain adaptation. In: ECCV. pp. 443–450. Springer (2016)
25. Tarvainen, A., Valpola, H.: Mean teachers are better role models: Weight-averaged consistency targets improve semi-supervised deep learning results. In: NIPS (2017)
26. Tzeng, E., Hoffman, J., Saenko, K., Darrell, T.: Adversarial discriminative domain adaptation. In: CVPR (2017)
27. Wang, J., Zhu, X., Gong, S., Li, W.: Transferable joint attribute-identity deep learning for unsupervised person re-identification. In: CVPR (2018)
28. Wei, L., Zhang, S., Gao, W., Tian, Q.: Person transfer gan to bridge domain gap for person re-identification. In: CVPR (2018)
29. Yang, F., Yunchao, W., Guanshuo, W., Yuqian, Z., Honghui, S., Thomas, H.: Self-similarity grouping: A simple unsupervised cross domain adaptation approach for person re-identification. ICCV (2019)
30. Yu, H.X., Zheng, W.S., Wu, A., Guo, X., Gong, S., Lai, J.H.: Unsupervised person re-identification by soft multilabel learning. In: CVPR (2019)
31. Zhang, J., Kalantidis, Y., Rohrbach, M., Paluri, M., Elgammal, A., Elhoseiny, M.: Large-scale visual relationship understanding. In: AAAI (2019)
32. Zhang, X., Cao, J., Shen, C., You, M.: Self-training with progressive augmentation for unsupervised cross-domain person re-identification. ICCV (2019)
33. Zheng, L., Shen, L., Tian, L., Wang, S., Wang, J., Tian, Q.: Scalable person re-identification: A benchmark. In: ICCV (2015)
34. Zhong, Z., Zheng, L., Kang, G., Li, S., Yang, Y.: Random erasing data augmentation. arXiv preprint arXiv:1708.04896 (2017)
35. Zhong, Z., Zheng, L., Li, S., Yang, Y.: Generalizing a person retrieval model hetero- and homogeneously. In: ECCV (2018)
36. Zhong, Z., Zheng, L., Luo, Z., Li, S., Yang, Y.: Invariance matters: Exemplar memory for domain adaptive person re-identification. In: CVPR (2019)
37. Zhu, J.Y., Park, T., Isola, P., Efros, A.A.: Unpaired image-to-image translation using cycle-consistent adversarial networks. In: ICCV. pp. 2223–2232 (2017)